Modelling Simul. Mater. Sci. Eng. **17** (2009) 055007 (10pp) doi:10.1088/0965-0393/17/5/055007

Motion of misfit dislocation in an Ni/Ni_3Al interface: a molecular dynamics simulations study

Hong-Xian Xie[1,4], **Chong-Yu Wang**[1,2,3] **and Tao Yu**[1]

[1] Central Iron and Steel Research Institute, Beijing 100081, People's Republic of China
[2] Department of Physics, Tsinghua University, Beijing 100084, People's Republic of China
[3] International Centre for Materials Physics, Academia Sinica, Shenyang 110016, People's Republic of China

E-mail: hongxianxie@163.com

Received 20 November 2008, in final form 25 May 2009
Published 23 June 2009
Online at stacks.iop.org/MSMSE/17/055007

Abstract

Motion of misfit dislocation in an Ni/Ni_3Al interface is studied in periodic simulation cells subjected to applied shear stress. Three different motion mechanisms of the misfit dislocation have been observed. The simulation results show that at low stress, the motion of misfit dislocation occurs through the nucleation and propagation of the double kinks; however, at higher stress, the motion of misfit dislocation is obstructed by an intrinsic stacking fault. The simulation results suggest that the stability of the Ni/Ni_3Al interface strongly relates to the interaction of the misfit dislocations that are perpendicular to each other.

(Some figures in this article are in colour only in the electronic version)

1. Introduction

Nickel-base superalloys are widely used for structural components in gas turbines for power generation and in aircraft. These alloys consist of a Ni-based matrix (fcc γ phase) with a dispersion strengthening phase, i.e. the ordered intermetallic precipitate particles of Ni_3Al ($L1_2$ γ' phase). Because the lattice parameters of the two phases are not identical, a stress field resulting from the lattice mismatch will be created [1]. Obviously, the interface with the stress field is unstable. Based on the principle of minimum energy, the atoms on the interface will rearrange in order to minimize the elastic stress field between the γ phase and the γ' phase, i.e. a self-accommodating process. So the misfit dislocations will be created in the interface. These misfit dislocations, that are edge in character and have a Burgers vector in the plane of the interface, widely exist in the single crystal superalloy and form dislocation networks [2, 3]. The dislocation networks can prevent slip dislocations in the γ channel from approaching or

[4] Author to whom any correspondence should be addressed.

cutting the network [4]. However, to our knowledge, few works have been done to study the motion of misfit dislocation in the γ/γ' interface.

Dislocations move through the crystal producing a permanent change in shape. Consequently, exactly how dislocations move in response to stress has been a matter of serious concern and intensive study [5–11]. There is a long-hypothesized kink-pair mechanism about the motion of dislocation [12]. Given that direct experimental observations of dislocation motion at the atomic scale are very difficult, molecular dynamics (MD) is the method of choice for exploring the mechanistic intricacies of dislocation motion. Chang *et al* [13, 14] simulated the motion of edge and screw dislocations in b.c.c Mo and concluded that at low temperature the edge dislocation moved primarily through kink nucleation, whereas the mobility of the screw dislocation was strongly facilitated by the presence of a kink. Marian *et al* [11] simulated the motion of the screw dislocation in b.c.c iron and presented visualization of the long-hypothesized kink-pair mechanism in action in MD. Using a high-resolution transmission electron microscope, the kink motion was observed in carbon nanotubes [15]. However, these works have been done in high-Peierls-barrier materials (b.c.c metals and covalent crystals). As we know, there are few works in the literature that provide evidence on the existence of the kink-pair mechanism in an Ni-base superalloy.

In this work, Ni and Ni_3Al are used in the modeling of the γ and γ' phase, respectively [16]; so the misfit dislocation in the γ/γ' interface of a Ni-base superalloy can be modeled by the misfit dislocation in the Ni/Ni_3Al interface. (It is natural for the real Ni-base superalloy that the γ phase is not pure Ni and the γ/γ' microstructure has small amounts of other elements such as Re and Co; the model presented is simplified in order to extract the fundamentals of misfit dislocation behavior.) The motion of misfit dislocation in the Ni/Ni_3Al interface under the applied shear stresses is studied using MD simulation. The atomic structure of the kink is obtained, and the supersonic and multiple kinks are observed. Furthermore, the different mechanisms of the motion of the misfit dislocation are discussed. The simulation results suggest that the stability of the γ/γ' interface is related to the interaction of the misfit dislocations that are perpendicular to each other. Because there is a vast interfacial region between the solid solution γ phase and the ordered γ' precipitates, the instability of the γ/γ' interface may affect the mechanical properties of Ni-base superalloys.

The outline of the paper is organized as follows: we present the modeling and simulation in section 2. Section 3 is devoted to a discussion of misfit dislocation's motion at applied shear stress and detailed simulation results. Finally, the simulation results and the main conclusions are summarized in section 4.

2. Modeling and simulation

The process of modeling can be divided into two steps. The first step is the construction of a model with misfit dislocation in the Ni/Ni_3Al interface. Both Ni and Ni_3Al possess face-centered-cubic structures; however, the lattice parameters of the two are not identical. When the mismatch of the lattice exceeds the limit of elasticity, the misfit dislocation will be formed in the interface to reduce the distorted energy of the system. Considering the concept of coincidence site lattice on the misfit interface, we can write such a relation as [16]

$$(n+1)a_{\mathrm{Ni}} = na_{\mathrm{Ni_3Al}},$$

where n is the n-fold of the lattice parameter, a_{Ni} and $a_{\mathrm{Ni_3Al}}$ are the lattice parameters of Ni and Ni_3Al, respectively. In this work, the lattice parameters of Ni and Ni_3Al are $a_\gamma = 0.352$ nm and $a_{\gamma'} = 0.3573$ nm [17], respectively, so we can obtain $n = 66$. This indicates that within the range of misfit interface formed by 66 Ni_3Al lattices and 67 Ni lattices, the stress induced

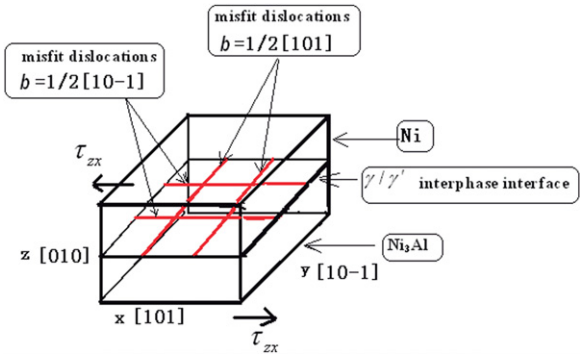

Figure 1. View of the MD simulation box used in the calculations. $\boldsymbol{b}$ is the Burgers vector.

by the difference in the lattice parameters should be relaxed. Based on the above analysis, we can construct a model with misfit dislocation in the Ni/Ni_3Al interface [16]. The simulation model with the (0 1 0) interface is oriented along the axes $x = [1\,0\,1]$, $y = [1\,0\,\bar{1}]$, $z = [0\,1\,0]$, and is divided into two parts by the (0 1 0) plane, including a total of 778 360 atoms. The top half-part is Ni_3Al, with box vectors 66[1 0 1], 66[1 0 $\bar{1}$] and 11[0 1 0], respectively; and the bottom half-part is Ni, with box vectors 67[1 0 1], 67[1 0 $\bar{1}$] and 11[0 1 0], respectively. The model is periodic along the x and y directions and has free surfaces as upper and lower bounds in the z direction. The Voter–Chen potential [17] is used, which is very successful in the study on the Ni–Al systems [16, 18–21]. The model is then relaxed by MD calculation of 2000 time steps, and the relaxation is carried out by integrating Newton's equations of motion [22] for all atoms using a time step of 5×10^{-15} s. Through the MD relaxation we can obtain the equilibrium atomic structure of misfit dislocation, which is located at the Ni/Ni_3Al interface which is square in shape and 16.68 nm in side length [16].

The second step is to activate the dislocation to move. In order to do this, shear stress τ_{zx} is applied through forces on several atomic layers at the free surfaces (see figure 1). During the simulation the same boundary condition and time step are used as the first step. The temperature of the system remains invariant (5 K) during the loading process, which is obtained by the velocity renormalization technique (at each time step every atom's velocity rescales by the same factor such that the total kinetic energy agrees with the equipartition value at the specified temperature). The size of the model in the z direction is doubled and it is found that there is no size effect on the results. Two measures have been taken to minimize the influence of the shock waves. The first measure is the velocity renormalization technique (temperature control). When the shock waves propagate through the system, the kinetic energy of the atoms will increase, and lead to an increase in system temperature. The velocity renormalization technique can weaken the influence of the shock waves by controlling the kinetic energy of atoms. The second measure is that a velocity damping term has been added before the misfit dislocation begins to move.

3. Results and discussion

At 5 K, the misfit dislocation begins to move under the stress $\tau_{zx} = 125$ MPa. Based on the potential energies of the atoms, we have selected the atoms with higher potential energies in the dislocation core area and along the dislocation lines to visualize the dislocation. The pattern of the misfit dislocations at 2.8 ps and under applied stress $\tau_{zx} = 501$ MPa is shown in figure 2.

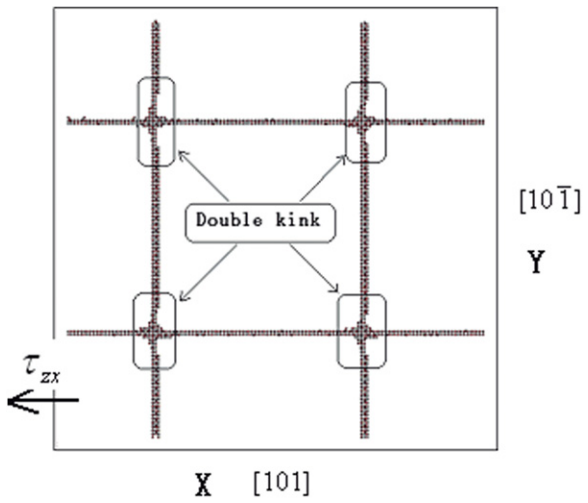

Figure 2. Double kinks nucleate at the intersection of the misfit dislocation lines. The time is 2.8 ps and the applied stress is $\tau_{zx} = 501$ MPa.

From figure 2, it can be seen that there are four double kinks formed at the intersections of the misfit dislocation lines. Using the technique of visualization, we have given a series of vivid snapshots of the double kinks nucleation and the propagation process in figure 3. In figure 3(b), a portion of the dislocation line jumps to the next lattice position (Peierls valley) forming a pair of atomic-sized kinks. Driven by stress, the kinks then rapidly migrate along the dislocation line (see figure 3(c)) and eventually recombine through the periodic boundary or oppositely signed kink. As a result, the entire dislocation translates to the next lattice position (see figure 3(d)). In order to display the structure of the kink clearly, the right-hand kink in figure 3(c) is enlarged, from which we can obtain the width and the height of the kink. In our simulation, the width of the kink is about $5b$ (b is the magnitude of the Burgers vector), which is consistent with the theoretical value ($3b - 7b$) [23–26], and the kink height is $1b$. The simulations show that at low stress, the kinks first are formed at the intersections of the misfit dislocation lines, then migrate along the dislocation line and eventually recombine with oppositely signed kink, leading to the entire dislocation moving forward a Burgers vector; that is to say, the mobility of the misfit dislocation is controlled by the double kinks nucleation and propagation process. Chang *et al* [13] have simulated the motion of edge dislocation in b.c.c Mo and concluded that at low temperature the edge dislocation moved primarily through the kink nucleation, Based on this work and Chang's work, we can conclude that the motion mechanism of the edge dislocation is not the same in different materials.

To probe why the double kinks initially nucleate at the intersection of the misfit dislocation lines, the potential energies of the atoms located at the dislocation core area and along the four misfit dislocation lines are plotted in figure 4. As can be seen in the figure, the potential energies of the atoms in dislocation cores but not at the intersections of the misfit dislocation lines are about -4.19 eV; however, the potential energies of the atoms which are located at the intersections of the misfit dislocation lines are about -4.02 eV; the difference between them is 0.17 eV. It is well known that higher potential energy leads to the weakening of interatomic bonds near the intersections of the misfit dislocation lines, and the kink nucleation enhancement is connected with a lowering of the Peierls barrier due to the weakening of interatomic bonds. So the double kinks will initially nucleate at the intersections of the misfit dislocation lines.

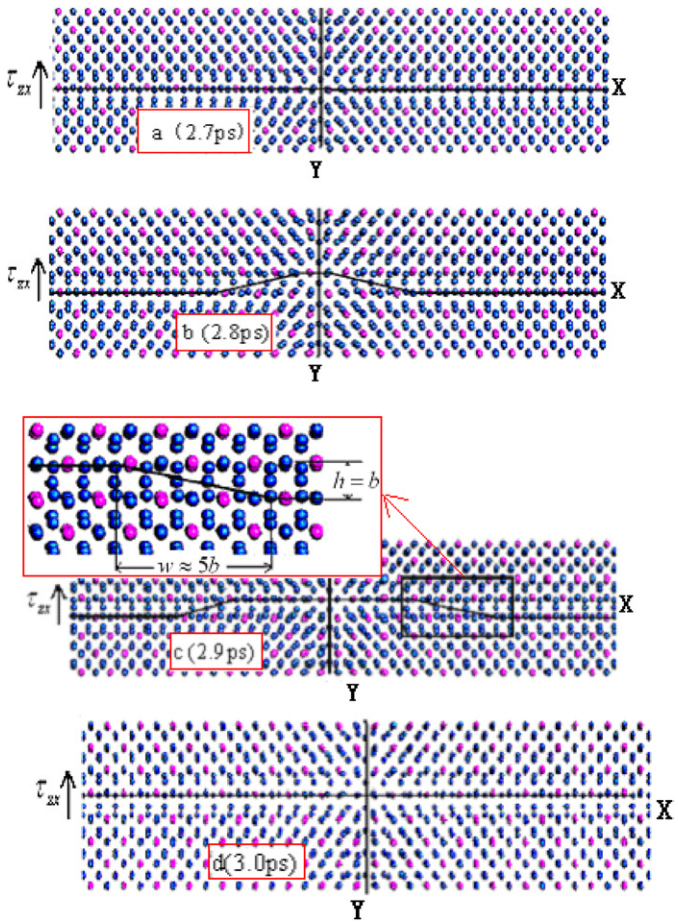

Figure 3. The double kinks mechanism of the dislocation motion at 5 K and under the stress $\tau_{zx} = 501$ MPa. The blue and pink balls represent Ni and Al atoms, respectively. (*a*) at 2.7 ps, the dislocation line lies along the initial Peierls valley; (*b*) at 2.8 ps, the double kinks have nucleated at the intersection of two misfit dislocations; (*c*) at 2.9 ps, the kinks have swept through about half of the dislocation line (*b* is the magnitude of the Burgers vector); (*d*) at 3.0 ps, the two kinks recombine with the other kinks in the next Peierls valley.

From the above analyses, we can know that the misfit dislocations on the Ni/Ni_3Al interface are easy to move due to the double kink's nucleation at the intersections of the misfit dislocation lines. Furthermore, there is a vast interfacial region between the solid solution γ phase and the ordered γ' precipitates [27], so the instability of the γ/γ' interface may affect the mechanical properties of the nickel-base superalloys.

In the following part, we focus on the relationship between the velocity of dislocation and the applied shear stress (see figure 5). From figure 5, it can be seen that the whole velocity–stress curve is divided into four pieces by the three points at which the applied shear stresses are 501 MPa, 3509 MPa and 7018 MPa, respectively. Therefore, we will study the mechanism of dislocation motion in each region.

When the applied shear stress is less than (or equal to) 501 MPa, the double kinks initially nucleate at the intersection of the misfit dislocations and migrate along the dislocation line, then mutually annihilate with the kinks from another pair. The new double kinks cannot be

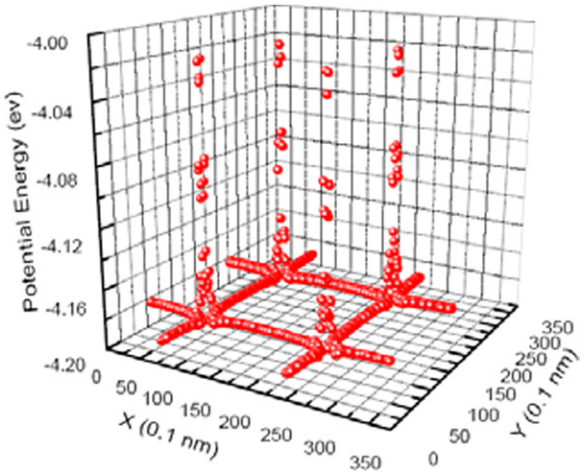

Figure 4. The potential energies of the atoms located at the four misfit dislocation lines.

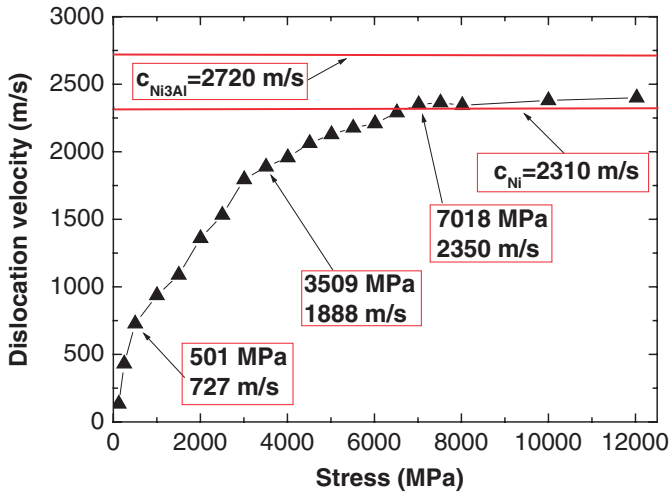

Figure 5. Misfit dislocation velocity as a function of the stress at $T = 5$ K. c_{Ni} and c_{Ni_3Al} are the transverse-sound-wave velocities in Ni and Ni_3Ai, respectively, which are calculated by the formula $c = \sqrt{\mu/\rho} = \sqrt{(C_{11} - C_{12})/2\rho}$, where μ is the shear modulus and ρ is the density, C_{11} and C_{12} are elastic constants which come from [17].

produced unless the old kinks annihilate with each other (see figure 3). The velocity of the kink can be calculated by equation [12]

$$v_k = \frac{l}{h} v_d,$$

where v_d is the velocity of misfit dislocation, h is the height of the kink and l is the interval of two kinks that are produced one after the other from the same point. From figure 3, we can obtain $h = b$ and $l = 33b$ (b is the magnitude of the Burgers vector), so the velocity of kink is 33 times the velocity of the misfit dislocation. Under the applied shear stress $\tau_{zx} = 501$ MPa, the velocity of kink is 23 991 m s^{-1}, which is about ten times the transverse-sound-wave velocity.

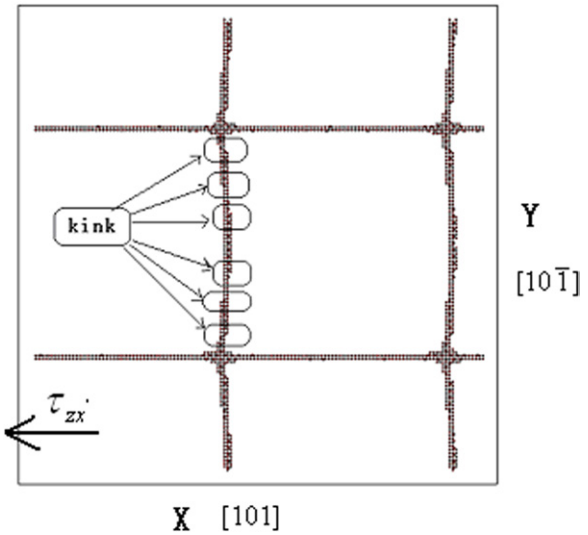

Figure 6. Multiple kinks have been formed on the dislocation lines under the applied shear stress $\tau_{zx} = 1003$ MPa at 13.1 ps. Kinks on a part of dislocation line are pointed out.

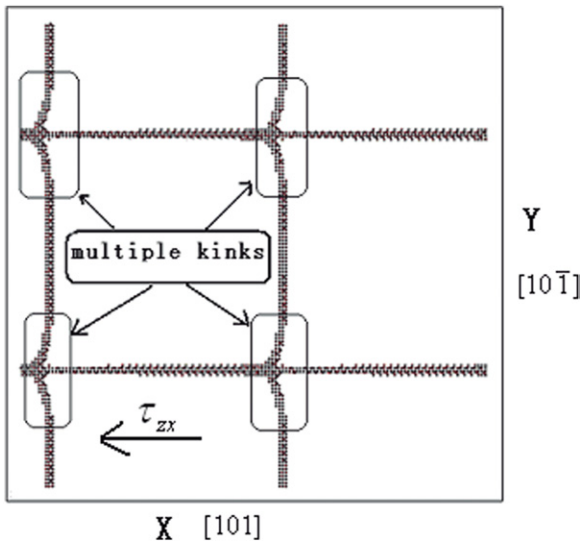

Figure 7. Multiple kinks only exist near the intersections of the misfit dislocation lines, but do not migrate along the dislocation line under the applied shear stress $\tau_{zx} = 6015$ MPa at 4.9 ps.

When the applied shear stress is between 501 and 3509 MPa, the double kinks also nucleate at the intersection of the misfit dislocations and migrate along the dislocation line. However, before mutually annihilating with the kinks from another pair, the new double kinks have nucleated and migrated along the dislocation line. So multiple kinks can be formed on the dislocation line (see figure 6).

When the applied shear stress is larger than (or equal to) 3509 MPa, the character of misfit dislocation motion changes dramatically (see figure 7). Therefore, multiple kinks only exist

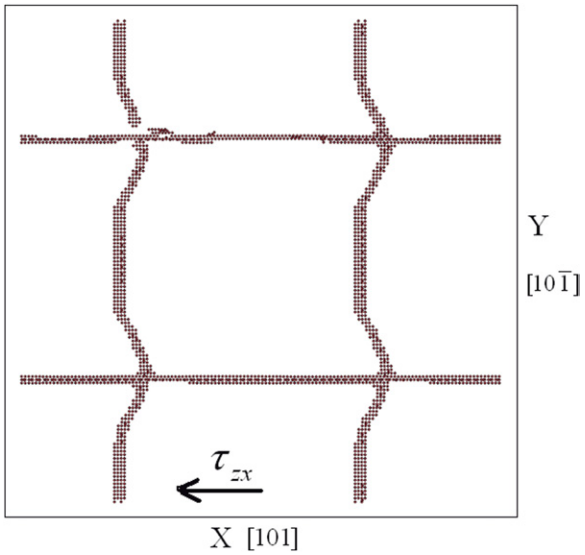

Figure 8. This part of dislocation at the intersection lags behind other parts of the moving dislocation under the applied shear stress $\tau_{zx} = 8021$ MPa at 15 ps.

near the intersections of the misfit dislocation lines, but do not migrate along the dislocation lines. The two misfit dislocations get over the Peierls barrier as a whole. So $\tau_p = 3509$MPa is the Peierls threshold stress that marks a transition between distinctly different mechanisms of dislocation motion: the kink-pair mechanism [12] below τ_P and the viscous phonon-drag mechanism [28] above τ_P. In the viscous phonon-drag mechanism, the motion of dislocation is not by the kink nucleation and the kink migration process but is characterized by a lattice damping (drag) effect, which is dominated by phonon drag.

We now come to the third dynamic transition under the higher shear stress (larger than or equal to 7018 MPa). During the initial time, the two misfit dislocations accelerate and get over the Peierls barrier as a whole. When the velocity of the dislocation reaches the value of the transverse-sound-wave velocity in Ni (see figure 5), the part of the dislocation near the intersection slows down and lags behind the other part of the moving dislocation (see figure 8), then the whole moving dislocation slows down. What causes this sudden change in the motion behavior? A meticulous analysis of the simulation snapshot under the stress of 8021 Mpa reveals the underlying mechanism. We have carefully studied the atomic configuration in front of the intersection of the misfit dislocation and displayed the results in figure 9. From figure 9(*a*) it is found that a half $1/6[1\,1\,2]$ dislocation loop, deriving from the misfit dislocation which is parallel to the x-axis, has been emitted on the$(1\,1\,\bar{1})$ plane; therefore a piece of intrinsic stacking fault has been formed (see figure 9(*b*)). The intrinsic stacking fault can obstruct the motion of the dislocation at the intersection. So the third dynamic transition can be attributed to the interaction between the moving dislocation and the intrinsic stacking fault.

4. Summary

In summary, the motion of misfit dislocation in the Ni/Ni_3Al interface under the applied shear stresses is studied by MD simulation. The atomic structure of the kink is given in detail and the width of the kink is obtained. Furthermore, the supersonic kink and multiple kinks are

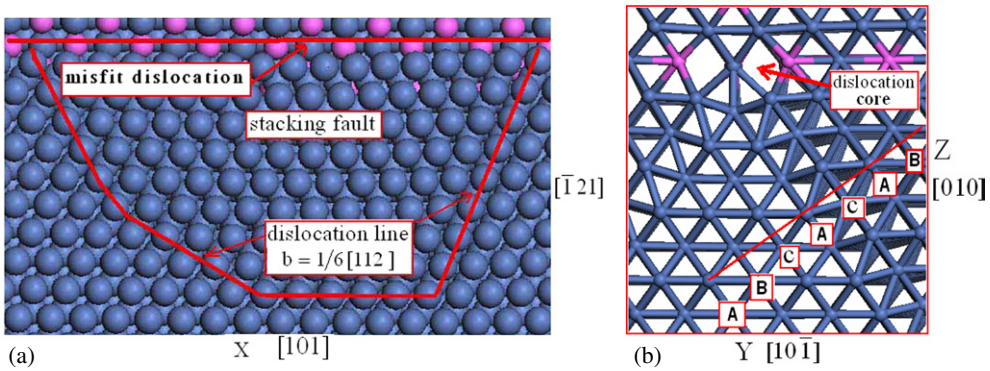

Figure 9. Formation of twin in front of the misfit dislocation at the intersection under the applied shear stress $\tau_{zx} = 8021$ MPa. The blue balls and pink balls represent Ni and Al atoms, respectively. (*a*) A piece of intrinsic stacking fault, which is surrounded by a half dislocation loop, has been formed on the (1 1 $\bar{1}$) plane (7 ps). (*b*) The intrinsic stacking fault forms ahead of the intersection of the misfit dislocations (7 ps), and the stacking sequence is . . . ABCACABC. . . ..

observed. Meanwhile, the relationship between the velocity of dislocation and the applied shear stress are studied. The whole velocity–stress curve is divided into four regions by the three points at which the applied shear stresses are 501 MPa, 3509 MPa and 7018 MPa, respectively; furthermore, the mechanism of dislocation motion in each region is carefully investigated. The simulation results show that at low stress, the motion of misfit dislocation occurs through the nucleation and propagation of the double kinks; however, at higher stress the motion of misfit dislocation is obstructed by an intrinsic stacking fault. Our simulation results suggest that the stability of the γ/γ' interface strongly relates to the interaction of the misfit dislocations that are perpendicular to each other. Because there is a vast interfacial region between the solid solution γ phase and the ordered γ' precipitates, the instability of the γ/γ' interface may affect the mechanical properties of nickel-base superalloys.

Acknowledgments

This research was supported by the National Basic Research Program of China (Grant No 2006CB605102) and the National Natural Science Foundation of China.

References

[1] Devincre B, Kubin L P, Lemarchand C and Madec R 2001 *Mater. Sci. Eng.* A **309–310** 211
[2] Lahrman D F, Field R D, Darolia R and Fraser H L 1988 *Acta Metall.* **36** 1309
[3] Gabb T P, Draper S L, Hull D R and Nathal M V 1989 *Mater. Sci. Eng.* A **118** 59
[4] Zhang J X, Murakumo T, Koizumi Y, Kobayashi T and Harada H 2003 *Acta Mater.* **51** 5073
[5] Bulatov V V, Abraham F F, Kubin L, Devincre B and Yip S 1998 *Nature* **391** 669
[6] Zhou S J, Preston D L, Lomdahl P S and Beazley D M 1998 *Science* **279** 1525
[7] Gumbsch P and Gao H 1999 *Science* **283** 965
[8] Diaz de la Rubia T *et al* 2000 *Nature* **406** 871
[9] Miguel M C, Vespignani A, Zapperi S, Weiss J and Grasso J-R 2001 *Nature* **410** 667
[10] Li J, Van Vliet K J, Zhu T and Yip S 2002 *Nature* **418** 307
[11] Marian J, Cai W and Bulatov V V 2004 *Nature Mater.* **3** 158
[12] Hirth J P and Lothe J 1982 *Theory of Dislocations* (New York: Wiley)
[13] Chang J, Cai W, Bulatov V V and Yip S 2001 *Mater. Sci. Eng.* A **309** 160
[14] Chang J, Cai W, Bulatov V V and Yip S 2002 *Comput. Mater. Sci.* **23** 111

[15] Huang J Y, Chen S, Ren Z F, Wang Z Q, Wang D Z, Vaziri M, Chen G and Dresselhaus M S 2006 *Phys. Rev. Lett.* **97** 075501
[16] Zhu T and Wang C-Y 2005 *Phys. Rev.* B **72** 014111
[17] Voter A F and Chen S P 1987 *High Temperature Ordered Intermetallic Alloys* (*MRS Symposia Proceedings* No 82) ed R W Siegel *et al* (Pittsburgh: Materials Research Society) p 175
[18] Wen M and Lin D 1997 *Acta Mater.* **45** 1005
[19] Rey C, Garcia-Rodeja J and Gallego L J 1996 *Phys. Rev.* B **54** 2942
[20] Farkas D, Roqueta D, Vilette A and Ternes K 1996 *Modelling Simul. Mater. Sci. Eng.* **4** 359
[21] Xie H-X, Wang C-Y and Yu T 2008 *J. Mater. Res.* **23** 1597
[22] Allen M P and Tildesley D J 1987 *Computer Simulation of Liquids* (New York: Oxford University Press) p 83
[23] Gehlen P C 1972 *Interatomic Potentials and Simulation of Lattice Defects* (New York: Plenum)
[24] Wüthrich C 1977 *Phil. Mag.* **35** 325
[25] Seeger A and Wüthrich C 1976 *Nuovo Cimento* B **33** 38
[26] Duesbury M S 1983 *Acta Metall.* **31** 1747
[27] Anton D L 1994 *Intermetallic Compounds* vol 2 ed J H Westbrook and R L Fleischer (New York: Wiley) p 3
[28] Alshits V I and Indenbom V L 1986 *Dislocations in Solids* vol 7 ed F R N Nabarro (Amsterdam: North-Holland) chapter 34